

SOLAR CYCLE VARIABILITY OF MARS DAYSIDE EXOSPHERIC TEMPERATURES: MTGCM INTERPRETATION OF MGS DRAG DATA. S. W. Bougher¹, T. McDunn¹ and J. M. Forbes², ¹U. of Michigan (AOSS Department, Ann Arbor, MI 48109-2143; bougher@umich.edu and tmcdunn@umich.edu), ²U. of Colorado (Department of Aerospace Engineering Sciences, Boulder, CO 80307; forbes@colorado.edu).

Introduction: Using densities derived from precise orbit determination (POD) of the Mars Global Surveyor (MGS) spacecraft from 1999 to mid-2005, the response of the Mars' exosphere (both densities and temperatures) to short and long-term solar flux changes was recently established [1-4].

The POD technique is similar to that used by Bruinsma and Lemoine [5]. Each density value is determined from analysis of Deep Space Network (DSN) observations over processing arcs with lengths of ~4-5 days, and normalized to a constant altitude of 390 km using the DTM Mars empirical model [5]. The MGS satellite was in a 93.7° inclination 1400-0200 LT sun-synchronous 370 x 437 km frozen orbit with periapsis confined to 40-60°S Latitude. Most importantly, the density values extracted represent averages over all longitudes, and are strongly biased towards dayside (LT = 1400) Southern Hemisphere conditions.

In order to evaluate the response of Mars' thermosphere to changes in solar flux, it is necessary to convert to exospheric temperatures (Texo) using a model (DTM-Mars). The change in the observed Texo over the solar cycle is illustrated in Figure 1. A least squared functional form of this solar cycle variation is given as follows:

$$Texo = 130.7 + 1.53 * F10.7 - 13.5 * \cos(Ls - 85^\circ)$$

The first two terms capture the impact of the 81-day mean F10.7-cm fluxes received at Mars, thus taking into account the impact of changes in heliocentric distance with season. An additional small "seasonal" effect is included (Ls term) to account for solar declination changes and their impacts on local insolation. Analysis thusfar indicates that the passage of dust events does not perceptibly influence exospheric densities or temperatures.

Figure 1 shows that the solar cycle variation of Mars dayside exospheric temperatures is far different than that of Earth [3,4]. From Mars aphelion/solar minimum (MIN) to perihelion/solar maximum (MAX) conditions (F10.7 ~ 32 to 115), Texo varies from ~185 to 310° K. The solid Mars line corresponds to the solar flux terms of the functional equation, with the Ls effects removed. The slope of this Mars line is $\Delta T / \Delta F10.7 \sim 1.5$, which means that the exosphere temperature changes by 1.5° K per solar flux unit re-

ceived at the planet. The corresponding curve for Earth is also indicated, and is not linear, showing a slope which varies from 2.9 at solar maximum to 4.2 at solar minimum. Clearly, the response of Mars' Southern Hemisphere daytime exospheric temperatures to long-term solar flux variability is about ~36-50% that of Earth.

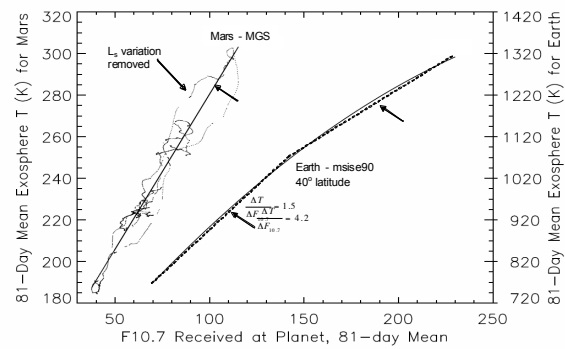


Figure 1: 81-day mean dayside exospheric temperatures at Mars and Earth over the solar cycle. From Forbes et al. [2007b].

Several processes determine Mars' exospheric temperatures and their variability [6,7]. These processes include: (1) solar EUV-UV fluxes producing heating, and its changes with solar cycle, solar rotation, distance from the sun, and local solar declination, (2) molecular thermal conduction, (3) CO₂ 15-micron cooling, and (4) adiabatic heating and cooling associated with global dynamics. According to Bougher et al. [6, 7], the primary balance occurs between EUV heating and molecular thermal conduction, with CO₂ cooling playing a minor role. In addition, Mars adiabatic cooling, due to rising motions on the dayside from the global circulation, should play a progressively more important role as the solar cycle advances. This "dynamical thermostat" cannot be ignored when examining the heat balances giving rise to solar cycle variations of dayside exospheric temperature.

Progress in the quantification of the relative importance of these heat balance mechanisms for maintaining Mars exospheric temperatures requires: (1) obtaining new measurements of O-abundances in the Mars thermosphere for constraining CO₂ cooling rates, and (2) systematic application of modern global dynamical models.

MGCM-MTGCM Formulation, Structure, and Inputs: Coupled Mars General Circulation Model (MGCM) plus Mars Thermospheric General Circulation Model (MTGCM) simulations are utilized that closely match MGS drag sampling conditions.

The MTGCM is a finite difference primitive equation model that self-consistently solves for time-dependent thermospheric neutral temperatures, neutral ion densities, and three component neutral winds over the Mars globe. The modern MTGCM code [8-11] contains prognostic equations for the major neutral species (CO_2 , CO , N_2 , and O), selected minor neutral species (e.g. Ar , O_2), and several photochemically produced ions (e.g. O_2^+ , CO_2^+ , O^+ , and NO^+ below 180 km). All fields are calculated on 33 pressure levels above 1.32 μbar , corresponding to altitudes from roughly 70 to 300 km (at solar maximum conditions), with a 5° resolution in latitude and longitude. The vertical coordinate is log pressure, with a vertical spacing of 0.5 scale heights. Key adjustable parameters which can be varied for MTGCM cases include the F10.7 or E10.7-cm index (solar EUV-UV flux variation), the heliocentric distance and solar declination corresponding to Mars seasons. A fast NLTE 15-micron cooling scheme is currently implemented in the MTGCM, along with corresponding near-IR heating rates [9]. These inputs are based upon recent detailed 1-D NLTE model calculations for the Mars atmosphere [12].

A simplified dayside photochemical ionosphere is formulated for the MTGCM, including the 4-major ions. Key ion-neutral reactions and rates are taken from a modern 1-D ionospheric model [13]; empirical electron and ion temperatures are adapted from the Viking mission for various solar conditions.

The MTGCM is driven from below by the NASA Ames Mars MGCM code [14] at the 1.32- μbar level (near 60-80 km). This coupling allows both the migrating and non-migrating tides to cross the MTGCM lower boundary and the seasonal effects of the expansion and contraction of the Mars lower atmosphere to extend to the thermosphere. Key prognostic variables are passed upward from the MGCM to the MTGCM at the 1.32- μbar level at every MTGCM grid point: temperatures, zonal and meridional winds, and geopotential heights. These two climate models are each run with a 2-minute time step, with the MGCM exchanging fields with the MTGCM at this frequency. No downward coupling is presently activated between the MGCM and the MTGCM. However, the impacts of lower atmosphere dynamics upon the upper atmosphere are dominant [10,11].

This coupled configuration has been validated using an assortment of recent Mars spacecraft observations employing thermosphere and ionosphere datasets [8-11]. For example, the global wind patterns simu-

lated by the MTGCM reveal a strong summer-to-winter inter-hemispheric Hadley circulation that is consistent with the seasonal variation of observed thermospheric winter polar warming features [9].

For analyzing MGS drag datasets, the MGCM and MTGCM input parameters are set as follows. F10.7 at Mars is varied from 25 to 110 units, corresponding to extreme MIN to MAX conditions. An EUV-UV heating efficiency of 22% (19%) is assumed initially (finally), based upon detailed offline heating efficiency calculations [15]. The MGCM lower atmosphere horizontal dust distribution is adopted from MGS TES mapping Year #1 [11].

Results and Conclusions: Simulated exospheric temperatures are selected and organized to match the MGS drag dataset sampling conditions. For each coupled MGCM-MTGCM simulation, Texo values are collected at $\text{LT} = 1400$ over all longitudes spanning the $40\text{-}60^\circ\text{S}$ latitude range. These values are averaged to remove longitude dependencies, in accord with the Mars exospheric temperatures plotted in Figure 1. Nine MGCM-MTGCM cases are examined initially (for 22% EUV efficiency). Cases were chosen that span the full range of F10.7 at Mars, and also provide representative seasonal variations of solar declination.

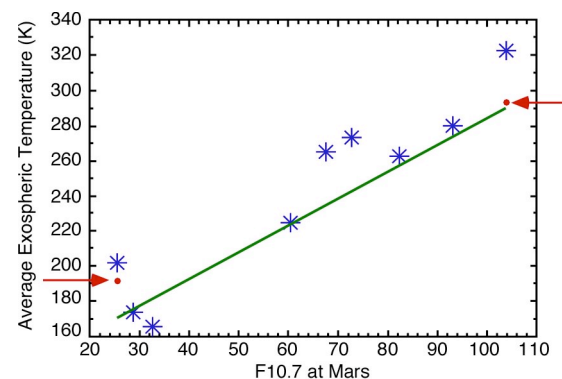


Figure 2: MTGCM simulated dayside exospheric temperatures over the solar cycle versus MGS drag temperatures. Green curve corresponds to Mars solid curve in Figure 1. Blue asterisks (red dots) correspond to MTGCM simulations using a 22% (19%) EUV-UV heating efficiency.

Figure 2 shows a comparison of MGS drag derived Texo values over the solar cycle (from Figure 1) with simulated Texo values for these nine cases. A “best” match of model and data values would be seen if the blue asterisks evenly straddled the green curve from lower left to upper right. This does occur for MIN conditions but not for MAX conditions. This implies that MGCM-MTGCM exospheric temperatures are too

warm by $\sim 10\text{-}25^\circ\text{K}$ for near MAX conditions. The corresponding slope of the mean simulated Mars response is $\Delta T/\Delta F_{10.7} \sim 1.64$. Two additional cases were conducted for MIN and MAX conditions (red dots), now utilizing a 19% EUV-UV heating efficiency. Little change occurs for MIN conditions, while Texo for MAX conditions cools by $20\text{-}30^\circ\text{K}$. The remaining seven cases for 19% efficiency will be conducted. However, we can conclude that a $\sim 19\%$ heating efficiency, within the limits of detailed offline calculations [15], provides an improved match of model and observed Mars exospheric temperatures over the solar cycle.

What thermal balances are responsible for these simulated variations of dayside exospheric temperatures? Figure 3 shows a map of exospheric temperatures at LT = 1400 over all longitudes/latitudes for MIN conditions. Notice cooler temperatures in Northern Hemisphere (summer) and equatorial latitudes, and warmer temperatures in Southern Hemisphere (winter) mid-latitudes ($30\text{-}60^\circ\text{S}$). This temperature distribution is consistent with a summer-to-winter inter-hemispheric global circulation, providing adiabatic cooling in summer latitudes, and adiabatic warming in winter latitudes.

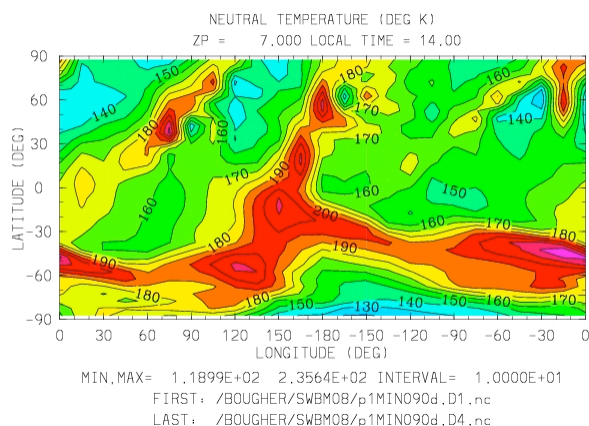


Figure 3: Coupled MGCM-MTGCM simulated dayside (LT = 1400) exospheric temperature map for MIN ($F_{10.7} = 25.5$ at Mars) conditions. Values range from a high of $200\text{-}240\text{K}$ (southern mid-latitudes) to a low of 140K (northern high latitudes). Temperature intervals are 10K .

Figure 4 illustrates heat balance terms for this same MIN simulation near the equator (cool temperatures). The major balance occurs between EUV heating and molecular thermal condition. CO_2 15-micron cooling effects are small at exospheric altitudes. However, adiabatic cooling and horizontal advection (resulting

from locally upwelling and diverging global winds) play a significant role in maintaining Texo.

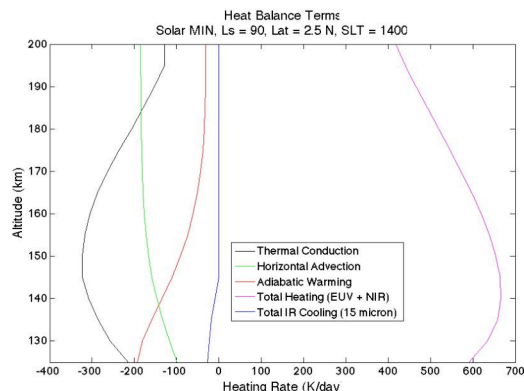


Figure 4: Coupled MGCM-MTGCM simulated equatorial dayside (LT = 1400) heat balance terms for MIN conditions. Curves are as follows: thermal conduction (black), EUV-UV heating (purple), CO_2 15-micron cooling (blue), adiabatic heating/cooling (red), hydrodynamic advection (green). Heating/cooling units are K/day.

Variations of dynamical heating/cooling terms with longitude and latitude can be significant. Figure 5 shows a map of adiabatic heating/cooling rates corresponding to the temperature map of Figure 3. It is clear that a very close match of Northern Hemisphere cool temperatures and adiabatic cooling rates (upwelling winds) exists, along with Southern Hemisphere warm temperatures and adiabatic heating rates (subsiding winds).

Similar thermal balance effects are seen throughout the solar cycle, with adiabatic cooling/heating rates intensifying in concert with increasing inter-hemispheric winds as MAX conditions are approached. Thus, we conclude that the influence of global winds must be carefully considered when investigating the thermal balances that regulate the solar cycle variation of Mars dayside exospheric temperatures [6, 7]. Future work entails a systematic study of these thermal balances throughout the solar cycle and their dependence on tidal and gravity wave influences impacting global winds patterns.

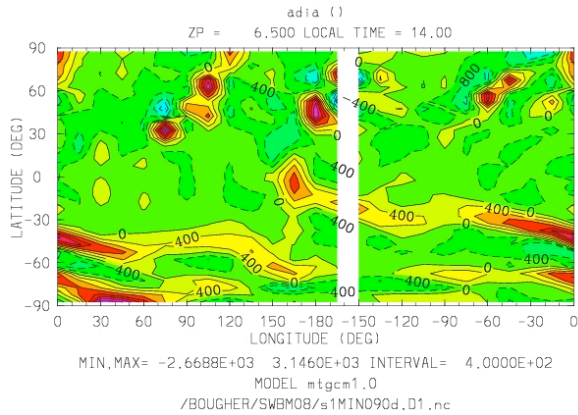


Figure 5: Coupled MGCM-MTGCM simulated dayside (LT = 1400) adiabatic heating/cooling map at exospheric altitudes for MIN conditions. Values range from a high of + 800-1200 K/day (southern mid-latitudes) to a low of -400-800 K/day (northern mid-latitudes). Heating/cooling intervals of 400 K/day are displayed. Compare this map to the exospheric temperatures in Figure 3.

References:

- [1] Forbes, J. M., Bruinsma, S., and Lemoine, F. G. (2006). *Science*, 312, 1366-1368.
- [2] Forbes, J. M. et al. (2007a). *J. Spacecraft Rockets*, 44, 1160-1164.
- [3] Forbes, J. M. et al. (2007b). *IUGG Abstract*.
- [4] Forbes, J. M. et al. (2008). *GRL*, 35, L01201.
- [5] Bruinsma, S. and Lemoine, F. G. (2002). *JGR*, 107, E10, 5085..
- [6] Bougher, S. W. et al. (1999). *JGR*, 104, E7, 16591-16611.
- [7] Bougher, S. W. et al.. (2000). *JGR*, 105, E7, 17669-17692.
- [8] Bougher, S. W. et al. (2004). *JGR*, 109, E03010.
- [9] Bougher, S. W. et al. (2006). *GRL*, 33, L02203.
- [10] Bougher, S. W. et al. (2008). *Sp.Sci. Rev.*, doi :10.1007/s11214-008-9401-9.
- [11] Bell, J. M et al. (2007). *JGR*, 112, E12002.
- [12] Lopez-Valverde, M. et al. (1998). *JGR*, 103, E7, 16799-16811.
- [13] Fox, J. L. and Sung, K.Y. (2001). *JGR*, 106, 21305-21335.
- [14] Haberle et al. (1999). *JGR*, 104, 8957-8974.
- [15] Fox, J. L. et al. (1995). *Adv. Sp. Res.* 17, (11), 203-218.